The Gamma Cube: a new way to explore the gamma-ray sky

François Lebrun, Régis Terrier, Damien Prêle, Denis Pellion, Dominique Ginhac, Remi Chipaux, Eric Bréelle, Philippe Laurent, Jean-Pierre Baronick, Alexis Noury, et al.

PROCEEDINGS OF SCIENCE

The Gamma Cube: a new way to explore the gamma-ray sky

François Lebrun[*,1], Régis Terrier[1], Damien Prêle[1], Denis Pellion[2], Dominique Ginhac[2], Remi Chipaux[3], Eric Bréelle[1], Philippe Laurent[1], Jean-Pierre Baronick[1], Alexis Noury[1], Christelle Buy[1], Christian Olivetto[1]

[1] *APC, AstroParticule et Cosmologie, Université Paris Diderot, CNRS/IN2P3, CEA/Irfu,*
Observatoire de Paris, Sorbonne Paris Cité,
10, rue Alice Domon et Léonie Duquet, 75205, Paris Cedex 13, France
E-mail: francois.lebrun@apc.univ-paris7.fr

[2] *Le2i, Université de Bourgogne, UMR CNRS 6306*
Allée Alain Savary, 21000 Dijon, France

[3] *CEA/DSM/Irfu/SEDI*
CE-Saclay, 91191 Gif sur Yvette Cedex, France

We propose a new concept to allow the tracking of electrons in a gamma-ray telescope operating in the 5–100 MeV band. The idea of this experiment is to image the ionizing tracks that charged particles produce in a scintillator. It is a pair creation telescope at high energy and a Compton telescope with electron tracking at low energy. The telescope features a large scintillator transparent to the scintillation light, an ad-hoc optical system and a high resolution and highly sensitive imager. The performance perspectives and the advantages of such a system are outstanding but the technical difficulties are serious. A few years of research and development within the scientific community are required to reach the TRL level appropriate to propose the Gamma Cube in response to a flight opportunity.

10th INTEGRAL Workshop: "A Synergistic View of the High Energy Sky"
15-19 September 2014
Annapolis, MD, USA

[1]Speaker

PoS(Integral2014)040

1. Introduction

Continuous gamma-ray emission in the 5–100 MeV domain results largely from high-energy particles interactions with matter (e^- bremsstrahlung, π^o, inverse Compton) or with magnetic fields through synchrotron emission. Particles are cosmic-rays or are accelerated locally in electric fields (pulsars), in shocks (SNRs, stellar winds, GRBs) or are channeled in jets (AGNs). If the magnetic field is highly ordered (pulsar, AGN jets, GRBs), the synchrotron emission is polarized. Flashes of continuous emission are produced in the earth atmosphere above stormy regions where electrons are accelerated to at least 100 MeV. Line emission is also expected in solar flares or from the low energy CR interactions with the carbon and oxygen nuclei of the ISM. The search at high gamma-ray energies for emission resulting from dark matter annihilation has been yet unsuccessful making more appealing a search at lower energies.

Such a rich domain has been only glimpsed with COMPTEL[1] and Fermi[2], the former being highly limited in sensitivity and the latter with no polarimetric capability and hampered by its angular resolution below 100 MeV. There is therefore a strong need for a polarimetric experiment offering both a good angular resolution and a high sensitivity in the 5-100 MeV range.

Since the emergence of grazing incidence mirrors and X-ray CCDs, X-ray astronomy underwent a fast and spectacular development leading to the present golden situation where the Chandra and XMM-Newton missions are successfully operating simultaneously since more than a decade. High energy gamma-ray astronomy with first the spark chambers (Oso-3, Sas-2, Cos-B, Egret) and then the Si stripped detectors (Agile, Fermi) made similar progresses as a result of the improvement in the particle tracking technique. At hard X-ray energies, the use of coded masks (Hexte, Granat, Integral, and Swift) allowed imaging but at moderate sensitivity even with the advent of room temperature semiconductor detectors. Above a few MeV only COMPTEL, the sole Compton telescope onboard a satellite (CGRO), provided significant results albeit with an SED sensitivity far behind its spectral neighbors. With the selection of Athena, a large X-ray mission as the next ESA cornerstone, and the advent of the next generation of ground based Čerenkov telescopes the contrast with the Comptel sensitivity will be outstanding.

The poorer sensitivity of the MeV experiments in comparison to its neighbors is largely due to instrumental difficulties specific to the domain. The lack of a mirror to form images on a large field of view and focus on a small radiation detector is probably the worst handicap. Above a few 10 MeV, pair creation is a very specific signature of a photon and provides immediate information about its incident direction. At lower energies, however, Compton scattering takes over and the corresponding signature in the detectors can be confused with charged particle interactions, while reconstructing the incident direction becomes harder. In addition, the interaction of photons with matter attains its minimum near 1 MeV so that photons at that energy are particularly difficult to detect. Finally, MeV is the domain of nuclear γ-ray lines, which makes it extremely interesting but gives it a strong instrumental background due to the activation of irradiated materials in space.

Compared to the pair telescope experiments, the Compton telescopes sensitivity is hampered by the absence of a real electron tracking capability; the direction of a gamma–ray photon being only restricted to a thick circle on the celestial sphere. The use of silicon DSSDs with low noise preamplifiers to get an accurate measurement of the energy deposits is expected to improve the sensitivity by a factor 30 or so. There is probably no way to go significantly beyond that point without an accurate tracking of the Compton recoil electron.

A Compton telescope with electron tracking is an experimentalist dream difficult to realize. The gamma-ray detection efficiency requires significant amounts of matter along the path of the photons but the electron tracking requires as little material as possible in between two successive electron position measurements. For example in a Compton telescope formed with a stack of Si DSSDs, the total Si length should be of the order of 15 cm to ensure a good Compton scatter efficiency at 5 MeV. On the other hand the thickness of a Si DSSD should not exceed 300 microns to ensure that the average scattering angle of a 5 MeV electron does not exceed 7°. Together these requirements imply a stack of 500 layers of DSSDs! If not excluded for excessive power consumption, heat dissipation or large fraction of dead material, it is certainly not reasonable from the cost point of view.

In the pair creation regime, the efficiency of the experiment is given by the converters. In these dense materials (lead, tungsten) the electrons suffer very heavy scatters that limit the angular resolution and preclude the use of the pair-creation plane for polarimetric studies. Gas TPC with their low density minimizing the electron scattering may be very efficient electron trackers. Here also the dead material is outside the detection volume. However, for a reasonable gas pressure (< 2 at), a good conversion efficiency requires large dimensions (~1 m) and the drift time for a reasonable high voltage (< 10 kV) is an issue for such a large TPC.

Clearly in both Compton and pair creation regimes what is missing the most is an accurate measurement of the electron tracks before significant scattering in the matter washes out their initial direction. .

2. Gamma Cube: the concept

A relativistic electron ionizes the matter along its track. The subsequent recombination may be accompanied by light emission (fluorescence). The direction of these fluorescence photons contains the information on the positions of the emitting atoms, i.e. the electron track. A proper optical system could form an image of the track that a very sensitive imager could record.

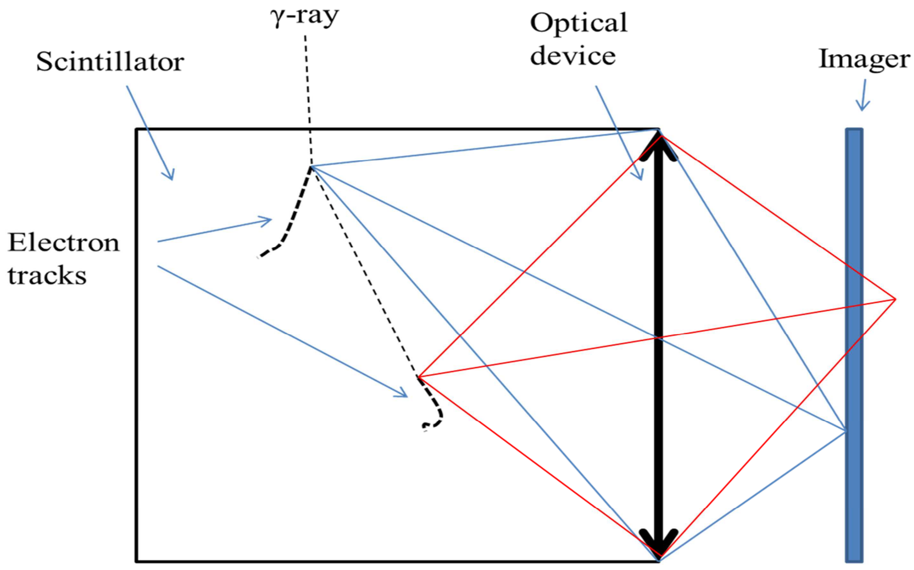

Figure 1: Schematic diagram illustrating the Gamma Cube: a scintillation tracker. A difficulty of the optical system is illustrated. If the optics focus the image of the first Compton electron track, it cannot at the same time focus as well the image of the second Compton electron track.

Figure 1 illustrates the principle; a gamma-ray photon of ~10 MeV undergoes two Compton scatterings, ejecting few MeV electrons, each of them producing a fluorescent track. A “lens” projects an image of these tracks on an imager. In the following, we will see that the detector part seems quite straightforward while there is interplay between the optical system and the imager readout and a tradeoff has to be performed to ensure the feasibility with interesting performance.

2.1 The detector

A proper electron tracking requires a material offering the lowest possible radiation length, i.e. a low density material with low Z. Such a requirement is exactly opposite to that for photoelectric absorption or pair creation, it implies a domination of the Compton scattering interaction and large dimensions to ensure a good efficiency. Fluorescence photons being the information carriers, we need as many as possible i.e. a scintillator offering a high light yield. However, not only a high light yield is required but the large dimensions require also a very transparent (at the fluorescence wavelength) medium to ensure the carriers reach the detector edges. The low density and transparency requirements point to plastic scintillators. The light yield is not very high but should be enough above 1 MeV. A plastic scintillator such as BC 408 (produced by Saint-Gobain) has the following characteristics:

- Made of light elements (polyvinyltoluene: C_9H_{10}).

- Its light yield is about 10 photons per keV with a wavelength of the emitted light around 420 µm and an absorption length around 4 m.
- It is available in large dimensions (meters) and its cost is moderate.
- It is a very fast scintillator (2 ns).
- It is robust, durable and can sustain space radiation.
- It is non-hygroscopic (no envelope needed) and can be shaped relatively easily.

For a Compton telescope, the spectral resolution is of prime importance as it governs the angular resolution and in the end the sensitivity. The moderate light yield of plastic hampers its use at low energy. Nevertheless a good light collection should allow sub-percent spectral performance above a few MeV if the 6 faces of the cube are similarly equipped with optics and imagers. For a large detector, the fastness of the plastic is a significant advantage to limit the dead time induced by the mandatory anticoincidence system. Its relatively low optical index should ease the light collection.

For a proper efficiency at 20 MeV, the size of the plastic cube should be around 60 cm. We will use that dimension in the following for sizing the experiment.

2.2 The optics

The main requirements on the optical system are a large depth of field, to properly image any part of the detector as well as a maximal photon collection because of weak luminosity of scintillation light. The first requirement is due to the impossibility to know a priori where the track will be located and because there will be several simultaneous tracks at different depths as illustrated on figure 1. Such requirements seem inaccessible to regular optics.

A camera able to focus a posteriori, at any chosen distance, exists. It is called a plenoptic camera [3,4] and allows performing digital light field photography (i.e. we measure both position and direction of photons reaching the imager). It features an array of micro-lenses, placed behind a simple large lens. Each micro-lens produces a small image of a part of the field on a large imager. The small images can be recombined to form images focused at various distances.

We investigate here a slightly simpler system for the gamma Cube using a single lens arrays placed on each side of the cube. Such a system allows a measure of the position and direction of scintillation photons reaching the surface of the cube. It is similar to a Shack-Hartmann beam analyzer.

The light produced by a track in the detector will be focused by lenses of the array on each side which will result in an array of track images on the imager (Fig 2a,b). The imaging process is then a two steps process: first determine the periods in the distribution of photons on the imager and then fold the various images produced with that period to obtain combined images (Fig 2d). This technique can be applied to the 3 pairs of sides of the cube to obtain a detailed 3D reconstruction of the event in the detector.

The size of the lenses, *s*, their focal length, *f*, and the imager distance from the cube faces, *h*, determine completely the optical properties of the system and must be chosen carefully. The error on the longitudinal position goes like s^{-1}, favoring large lenses, but one has to have a sufficiently large number of images to determine the period on the imager and to keep a focal to diameter ratio large enough to limit aberration effects. Similarly, a good lateral position reconstruction is obtained when the imager distance is such that the focus is made at ¾ of the cube depth. The typical resolution (separation power) achieved within the cube is around or below ⅓ of the lens diameter and localization accuracy that can easily go below the mm for energy deposits are the MeV level. We have found that lens size around or below the centimeter to be a good compromise.

With the capability to locate interactions down to the MeV level, the setup will have a low energy threshold of a few MeV for gamma-rays. The high energy limit will come from confusion: if the size of the track image exceeds the lens field of view, the images produced by neighboring lenses will start merging. A possible way to improve on this is to use a fully plenoptic system made of two lens arrays (a macroscopic and microscopic one).

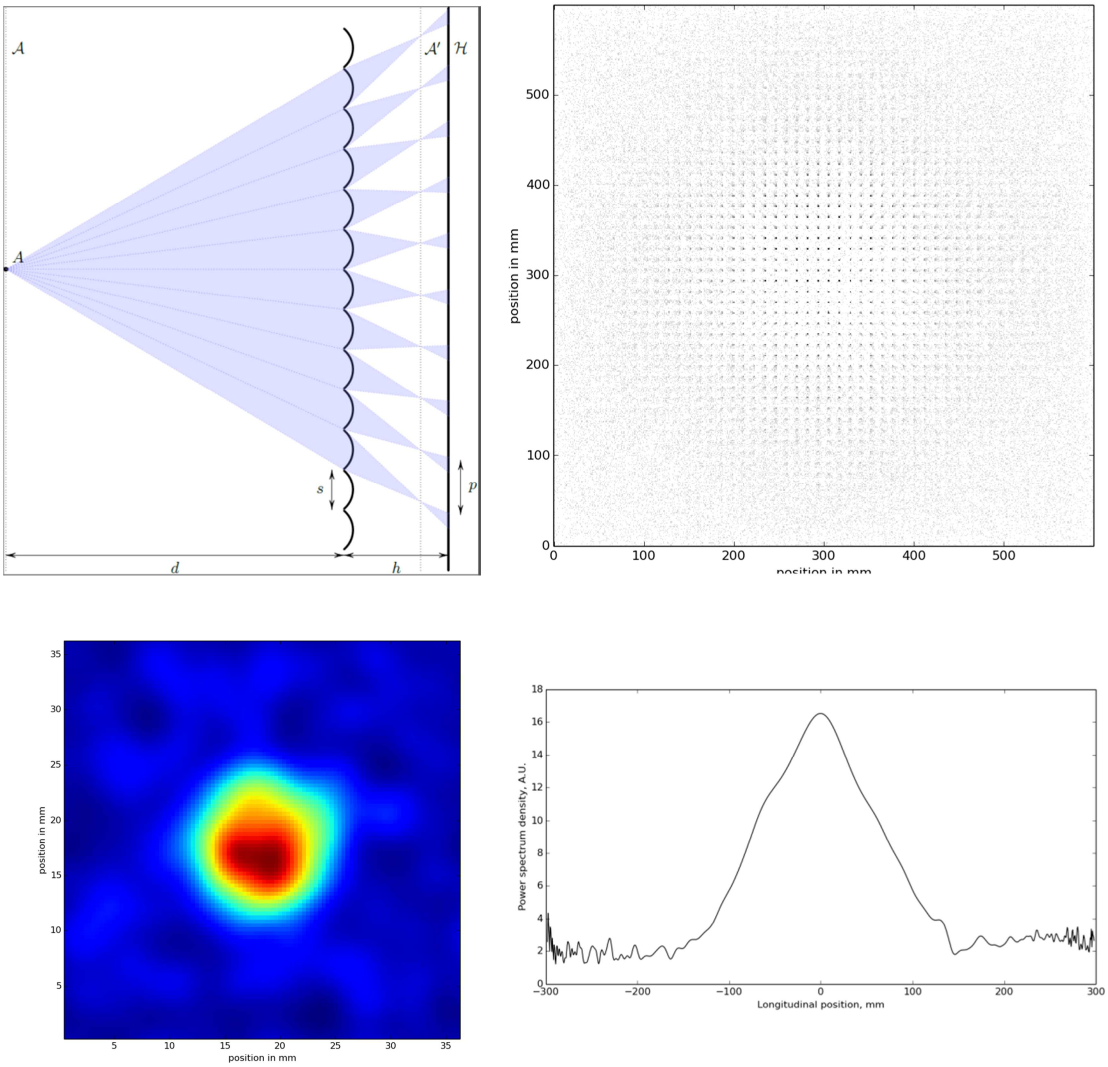

Figure 2

a) (top left) Geometry of the setup: A point source illuminates the lens array of square mesh which produces an array of images on the imager. The period p is directly connected to the lens array period s and the depth of the point source in the cube

b) (top right) The surface density of photons produced at the centre of the cube and focused by the lens array on one side of the cube. The period p is clearly visible

c) (bottom right) To obtain the period one can study the power spectrum density of X and Y positions of photons detected on the imager. Here we show the periodogram, i.e. the power spectrum density as a function of the depth in the cube for a point like emission at the centre of the cube releasing as many photons as a 1 MeV energy deposit. The peak gives the most probable position.

d) (bottom left) Once the period p is known one can fold the large image to obtain an image of the event inside the cube along the transverse direction. Here is shown an example of such a phasogram for the same event.

2.3 The imager

The requirements for the imager are the capability of detecting every fluorescence photon, a spatial precision sufficient to preserve the accuracy provided by the optics and a limited dark count rate (DCR). In principle, there are two possible regimes, one where the average number of events per pixel (the photon density) exceeds unity and the other where the photon density is significantly lower than one. In the former case, the number of photons per pixel has to be measured by pulse height, in the latter case we only need to register the addresses of the hit pixels. Pulse height measurement is so power consuming that it seems hardly applicable to a space experiment with a huge number of channels. For that reason only the latter case was investigated here.

A Single-Photon Avalanche Diodes (SPAD) is an extremely sensitive photo sensor, a photodiode operated in Geiger mode. Geiger mode provides internal gain as large as 10^6 carriers/photon, with very low power consumption (few 10 µW/mm^2). Indeed, a unique electron-hole pair generated by the absorption of a single photon leads to one million carriers. This huge multiplication is due to a self-sustaining avalanche process: successive impact ionizations of carriers accelerated by an electric field, above the breakdown threshold. So, the diode reverse current rises to a few mA in a few ns as it may occur across a switch going from OFF to ON state. Such a non-linear/binary regime allows a “digital” detection of single photon. The increasing current also crosses a quenching circuit (Fig. 3) placed in series with the voltage biasing, lowering the electric field effectively applied to the SPAD below the breakdown threshold. That turns OFF the avalanche process in a few 10 ns (reset time). Without self-sustaining avalanche process and until there is a new incoming photon, the current drops below 1 pA (leakage current) and the SPAD electric field is restored above the breakdown threshold. After this current pulse, SPAD is ready to detect a new photon.

A high-resolution - few 10 µm - imager sensitive to a single photon is actually developed by using an array of SPADs with a standard CMOS micro-electronic technology (AMS Opto CMOS 0.35 µm) [5]. Summation of Single Photon Avalanche photo Diode array signals allow efficient calorimetry and are known under the name of SiPM (Silicon Photo-Multiplier). However, imaging requires many readout channels, possibly as much as the number of SPADs. So, for a SPAD imager, a multiplexing technique must be considered. Analog multiplexing technique could be considered [6]. However the linear circuits used for analog multiplexing are power consuming and thus not compatible for space applications. Hence, it may be preferable to convert the SPAD detection of a photon [7] to digital signal in order to investigate a digital multiplexing/coding made by low power consumption CMOS circuitry. Based on such consideration, the pixel is composed of a single SPAD or a few of them (the photon density must be significantly lower than one), high voltage sources (HV = few 10V), a “quenching” circuitry and a 1-bit Analog to

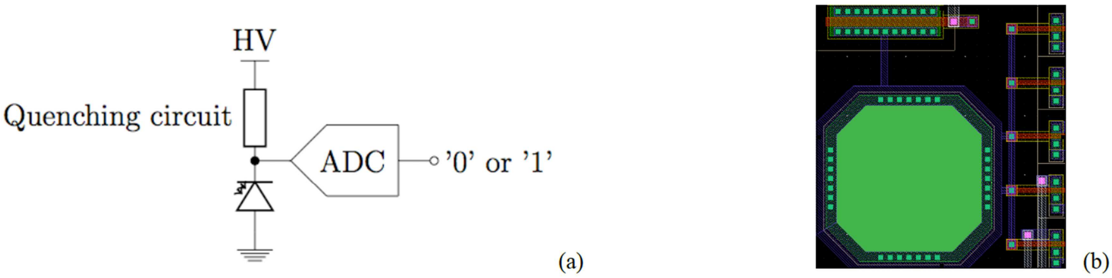

Figure 3

a) (left) Elementary cell (pixel) of a digital readout SPAD array.

b) (right) Layout of the cell demonstrator developed on a BiCMOS technology with coding circuit. On the top of the layout, the quenching circuit is a MOS transistor allowing an adjustment of the quenching resistance for the purpose of this demonstrator. On the right of the layout, 5 triggers act as “1 bit” ADC addressing a 5 wires bus used for coding the address of each pixel.

Digital Converter (ADC). The quenching circuit could be a simple resistor or a MOS transistor in ohmic regime used to find the optimum quenching resistance of our prototype. The 1-bit ADC is obtained using a simple comparator (a MOS transistor). It detects a decreasing of the voltage across the photo-diode. Using this single pixel scheme, coding of a sub-array system could be achieved. The output of the ADC of each pixel is copied on a digital bus following a standard binary code as shown in each line of figure 4a (top). Indeed, the binary code obtained at the end of the line provides the address of the hit pixel only if there is only one pixel hit at one time. So, a small array must be considered to “statistically” avoid simultaneous events. For a low photon flux application, this could still correspond to more than one hundred pixels. So, an array of SPAD could quickly image the flash of light produced in a fast scintillator to track particle interactions. However, a SPAD is not only triggered by incident photons. Even without any optical event, some thermally generated carriers produce also current pulses. The rate of these “dark” events (DCR) increases with the temperature and with the applied electric field. For this reason the SPAD array is passively cooled-down below 0 °C. Moreover, a coincidence (“Coinc” in Fig. 4a) detection correlated events allows to drastically reduce the impact of the dark count rate on the dead time and the data transmission rate. This coincidence could be obtained by analog or digital summation of each SPAD signal as is schematically represented in figure 4a. Indeed, the address of the hit pixel is only taken into account and propagated if a coincidence (real event – not dark) is detected by several sub-arrays.

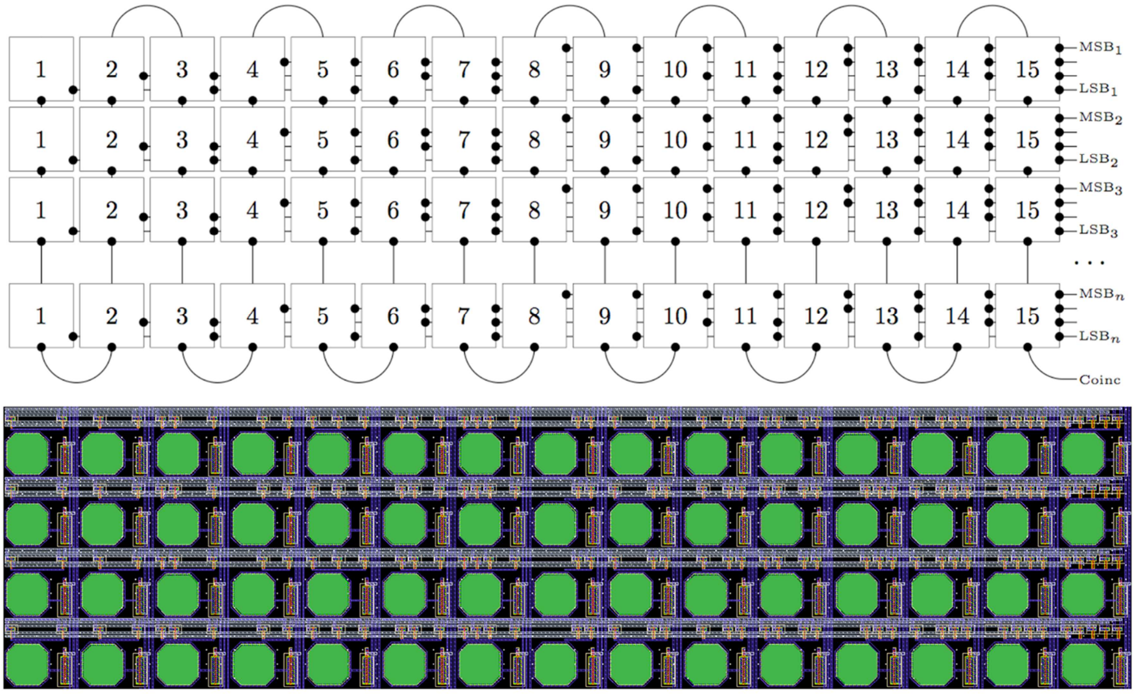

Figure 4

a) (Top) Representation of a SPAD array composed of “n” lines of 15 SPADs sub-array. The “Coinc” signal allows reading only simultaneous-event addresses.

b) (Bottom) Layout of a part of a prototype SPAD array following the discussed 4 bit digital coding + coincidence signal.

A 30 x 30 SPAD array demonstrator has been developed with 13 µm pixels and a digital coding. This prototype has been developed to characterize SPAD sensors on this 0.35 µm Opto BiCMOS AMS technology. Indeed, many geometries and topologies of SPAD have been designed. Moreover, A SPAD array with coding circuit would demonstrate the multiplexing capability achievable on such a technology.

A small pixel size is desirable to avoid losing image accuracy and the DCR per unit area decreases with the pixel size. However, the relative dead area increases when the pixel size decreases and the smaller the pixel, the larger is the pixel address and the longer is the readout. For an expected trigger rate of several thousand per second, the readout time should be kept below 10 µs to avoid significant dead time. In the end, a pixel size as large as 100µm could appears as a reasonable tradeoff.

3. Physics and event reconstruction

The tracks in 3D have first to be reconstructed before any attempt to retrieve the incident gamma-ray photon properties (energy, direction, polarization). To study this reconstruction we have performed simulations using the optical module of GEANT 4 to simulate the effect of a simple micro-lens array.

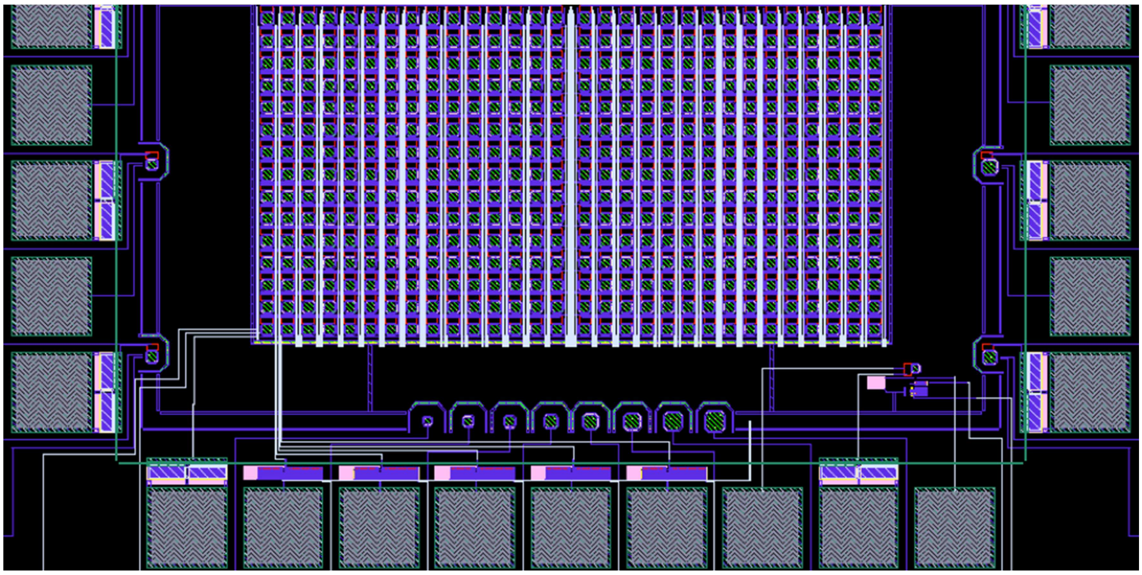

Figure 5

Layout of a part of the 30x30 SPAD array demonstrator. This array is composed of 15 pixels sub-arrays, which addresses a 4 bits bus. A latch registers kip information of each hit pixel address. Data of the full array is readout through a series output stream. Many test vehicles are placed all around the main array to characterize this technology: “AMS CMOS opto 0.35µm”.

These simulations have shown that about 70% of the photons emerge from the cube and around 35% are detected and can be used for calorimetry. Only 25% are detected and properly focused.

3.1 tracks reconstruction in 3D

Each element of the micro-lens arrays produces a clear cut image of an emitting point inside the cube. On each of the 6 faces, a square mesh of images is produced. The photon density over the cube face is maximal at the projected position of the source. The photon distribution over each imager provides an estimate of the source position with an accuracy at the level of the lens element size. Near the projected position, where optical conditions are optimal, the mesh is square and its size is equal to the lens-array element size times $1 + n\,h/d$, where h is the distance between the imager and the micro-lens array, d is the source distance from the micro-lens array and n is the refractive index of the array (which is assumed to be identical to that of the scintillator cube). The mesh is therefore a measure of the source longitudinal distance d. A 2-D Fourier transform of the image easily provides this mesh with a remarkable accuracy even at low energy where photons are scarce. Alternatively, with less demanding computing resources, the power spectra of two 1-D transforms can be summed and provides the same result (see Fig. 2c).

Once the mesh is known, the global image is folded to reveal the source image as would be produced by a central lens but with very high statistics (Fig.2d). In principle, the 6 images should be processed simultaneously since the mesh of one image is linked to the pattern center of 2 other images.

3.2 Efficiency and photon reconstruction from tracks

A gamma-ray photon can undergo a large number of scatters and not even lose all its energy since in the Thompson regime ($E < m_e c^2$) the average loss per interaction is very low. This is illustrated in Figure 6 where a few long tracks (red and blue) are clearly visible while in most scatterings the energy deposit is not visible.

These small energy losses are invisible since they hardly exceed a few tens of keV. Images in the Cube would be limited to the red and blue tracks. Practically the reconstruction of an interaction requires individual energy deposits greater than about 200 keV and a total energy deposition greater than 90% of the incident energy (given by the calorimetry). This requirement limits strongly the efficiency at low energy

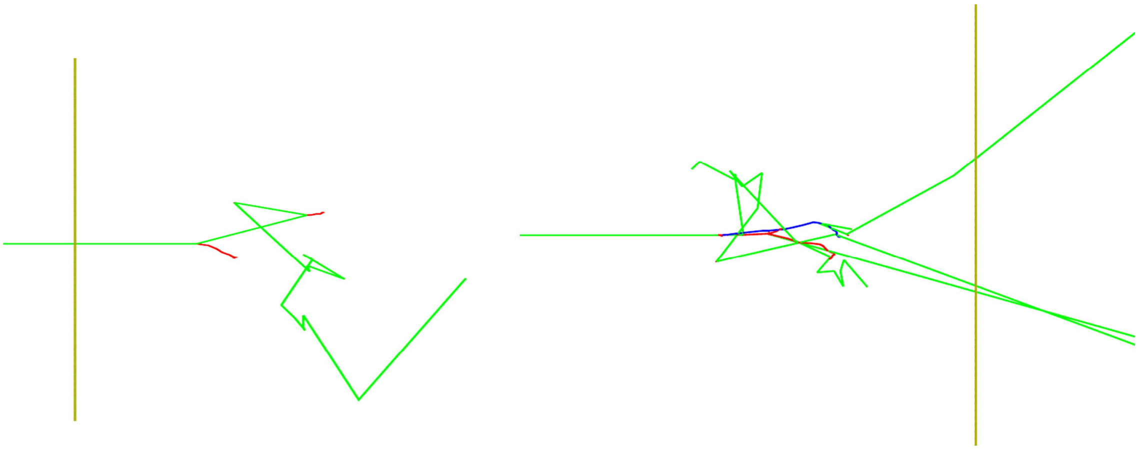

Figure 6

Tracks produced in the Gamma Cube by two gamma-rays coming from the left, a 10 MeV photon undergoing 2 Compton scatterings (Left) and a 50 MeV photon creating a pair (Right). Photon paths are in green, electron tracks are in red and positron tracks are in blue.

and acts as an implicit low threshold. With this requirement and adding the need of at least 2 interactions for a Compton scattering, one can compute the efficiency of the cube with GEANT 4 simulations that is illustrated in figure 9 in [8].

4. Orbits and background

4.1 Orbit merits and Background

The performance of an experiment such as the Gamma Cube depends strongly on the chosen orbit. On the one hand, an equatorial Low Earth Orbit (LEO) offers the lowest internal background but on the other hand the atmospheric gamma-ray emission may compensate and the field of view is reduced compared to a Highly Eccentric Orbit (HEO). Moreover, on a LEO the available power is less, the thermal control is more complicated and the telemetry may be an issue, especially if the experiment must generate alerts in real time (e.g. GRBs). If one considers placing the Gamma Cube at L2, the background and the field of view are the same as for an HEO but the telemetry requires the use of an expensive pointing antenna. It is therefore necessary to address carefully all these points. This cannot be done here but at least we can focus on the background issue and in so doing, we assume the L2 case is covered by the HEO study.

4.2 Gamma Cube background simulations

The background of the Gamma Cube has been simulated with the MEGAlib software toolkit. In this model, the telescope is composed of a cubic plastic scintillator (C_9H_{10}) of 60 cm by side, placed upon an aluminium satellite platform. Aluminium density has been adjusted to have a 500 kg platform. Two orbit types have been considered, LEO and HEO. The LEO is a typical equatorial low-Earth orbit at an altitude of 550 km; the main background contributions in that case are the Earth albedo, the Cosmic Gamma-ray Background (CGB), and the radioactivity induced by highest energy protons able to pass through the Earth magnetosphere. HEO is an orbit placed well above the radiation belts; in that case, the main contributions are the CGB and the radioactivity induced by cosmic protons. The result is shown in figure 10 in [8], where we can see the background spectra in the two cases; we could see also the background in a LEO, when we can discriminate and remove all the background induced by the Earth albedo. In this optimistic case, the background count rate above 1 MeV is reduced from 2350 s^{-1} down to 400 s^{-1}. From the background point of view a LEO is clearly the preferable orbit since the HEO background rate is about 5000 s^{-1} and cannot be reduced. LEO background is highly dominated by the Earth albedo contribution whereas the HEO one is dominated by the induced radioactivity, mostly coming from the ^{11}C, ^{22}Na, ^{24}Na and ^{26}Al isotopes created in the cube and platform respectively. Induced radioactivity is lower in LEO due to the geomagnetic cut-off.

5. conclusions

In principle, the Gamma Cube presents many conceptual advantages over other Compton or pair creation telescopes. It allows the imaging of electron tracks and the determination of the electron direction (Bragg peak). With this, ordering the gamma-ray interactions is much easier. There is no passive material within the detection volume where electrons or photons may interact without notice resulting in wrong gamma-ray reconstruction. The spatial resolution can be adapted to the needs by appropriately tuning the optics and the imager resolution. The number of readout channels is proportional to the detector area rather than its volume and since there is no A/D conversion, the power consumption per pixel is of the order of 1 µW with no heat dissipated in the detector.

A good fraction of these advantages should translate into an exceptional performance since the efficiency should be an order of magnitude better than COMPTEL (for a weight an order of magnitude lower), the background rejection is expected to be far superior and the angular resolution should be mostly limited by the electron scattering that in a plastic scintillator is nearly minimal. All these should result in a very good sensitivity in the 5–100 MeV range. In fact, the Gamma Cube is fully compliant with the seven aspects given as guidelines for the next generation of Compton telescopes[9].

However before this becomes a reality serious issues have to be tackled. First of all, a large SPAD array has to be realized with the ad hoc readout scheme. The main difficulty comes from the large size of the imagers that must be read in about 10 microseconds. Another difficulty here is the pixel dead zone that should be kept to a minimum. Also cooling will certainly be necessary to maintain the SPAD dark rate to an acceptable level. The optical system deserves a deep study based first on simulations. A system based on a single micro-lens array falls short in providing the requested dynamical range. A more complex system using several plenoptic cameras looks promising but has not yet been studied in detail. The 3D track reconstruction is feasible on ground but it might be different to perform it in less than a millisecond or so with a space qualified processor.

None of these difficulties appears as a hard point but they all require a lot of work that is justified by the outstanding advantages and expected performance.

References

1. Schoënfelder, V. et al., “Instrument description and performance of the imaging gamma-ray telescope COMPTEL aboard the COMPTON gamma-ray observatory”, Ap.J.Suppl., 86, 657 (1993)
2. Atwood, W.B. et al., “The Large Area Telescope on the Fermi gamma-ray space telescope mission”, Ap.J. 697, 1071 (2009)
3. Ng, R., Levoy, M., Brédil, et al, “Light Field Photography with a Hand-held Plenoptic Camera”, Stanford Computer Science Technical Report 2005-02 (2005).
4. Lumsdaine, A. and Georgiev, T., “The focused plenoptic camera”, IEEE International Conference on Computational Photography (ICCP), pp 1–8 (2009).
5. Jradi, K., Pellion, D. and Ginhac, D., “Design, Characterization and Analysis of 0.35µm CMOS Single Photon Avalanche Diode", Sensors 2014, 14, 22773-22784; doi:10.3390/s141222773
6. Dey, S., Banks, L., Chen S.-P. C., Xu, W., Lewellen, T., Myaoka, R., and Rudell, J, “A CMOS ASIC Design for SiPM Arrays”, IEEE Nuclear Science Symposium Conference Record, NP2.S-53, pp 732–737 (2011).
7. Burri, S. and Charbon, E., “SPAD Image Sensors: from Architectures to Applications”, in “Imaging Systems and Applications”, Monterey, California United States, ISBN: 1-55752-947-7. http://dx.doi.org/10.1364/ISA.2012.ITu4C.1 (2012).
8. Lebrun, F. et al., “The Gamma Cube: a novel concept of gamma-ray telescope”, Proc. SPIE 91440B (2014).
9. Schönfelder, V., “Lessons learnt from COMPTEL for future Telescopes”, New Astronomy Reviews, Vol 48, Issue 1-4, pp 193-198 (2004).

PoS(Integral2014)040